Acta Avionica

Volume XVII, 32-No.2, 2015

# MAGNETOMETER CALIBRATION USING ONE-LAYER NEURAL NETWORK

**Tomáš KLIMENT*, Dušan PRASLIČKA**
Faculty of Aeronautics, Technical University of Košice, Rampová 7, 041 21 Košice, Slovak Republic
**Corresponding author*. E-mail: tomas.kliment@tuke.sk

**Summary**. The paper presents a novel easy-to-use iterative calibration algorithm for a magnetic field estimation accuracy improvement, which can be successfully applied to the estimation of a 3-axis magnetometer biases and scale factors of the each axis, extended to estimate non-linearity and non-orthogonality corrections. The theory is based on the neural network that creates an inverse function the uncalibrated sensor's transfer function. Learning process of the neural network uses a gradient methodology applying total differential on the scalar error equation. The analyzed theoretical principles are supplemented by simulations and experimental measurements. The performed simulations and experiments confirmed that the algorithm successfully converges to a good estimation of the calibration constants. Other advantage of this methodology is that the calibration procedure is based on the attitude independent sensor discrete random rotation in the 3D space without the need of any non-magnetic calibration platforms. Advantages of this method compared with others lie not only in the simplicity of the presented algorithm, sensor attitude independency, measurement repeatability and no need of non-magnetic calibration platform utilization, but also in the speed, precision, undemandingness and comfort of the presented calibration procedure, which lead to the effective magnetometer calibration constants determination and calibration errors reduction.

**Keywords:** magnetometers; calibration; non-linearity; non-orthogonality

## 1. INTRODUCTION

Calibration of magnetic field sensors leads to the significant improvement of the sensor's accuracy, therefore many authors have developed various calibration methods for calibration constants determination [1-5,7]. The goal of the presented calibration methodology is to derive an easy-to-use calibration algorithm that can be used for a magnetic field estimation accuracy improvement. The paper presents a novel iterative calibration algorithm, which can be successfully applied to the estimation of a 3-axis magnetometer biases and scale factors of the each axis, extended to the estimation of non-linearity and nonorthogonality corrections.

## 2. THEORY

The calibration methodology is based on the one-layer feedforward neural network consisting of three adaptive elements, learning mode for the network training and working mode used for measured data correction. The neural network creates an inverse sensor's transfer function of the sensor. Post-proccesing is used for calibration. In first step magnetometer data are measured and then these data are used as a training set. This set of data are used repeatedly. Considering a 3-axial sensor of vector field with the bias, sensitivity, linearity and orthogonality errors, then during the repeated measurements we get for every step of measurement normalized $x^k$, $y^k$ and $z^k$ values representing uncalibrated almost orthogonal decomposition of the measured field vector in $x$, $y$ and $z$ axis, the scalar value $T$ of which can be calculated as:

$$T^k = \sqrt{\left(x^k\right)^2 + \left(y^k\right)^2 + \left(z^k\right)^2} \tag{1}$$

The error ε can be hence defined as a difference between the true scalar value of the magnetic induction vector normalized to 1, and the calculated value of the $T^k$ of the given *k* step:

$$\varepsilon^k = 1^2 - \left(T^k\right)^2 \tag{2}$$

For the each step of calibration the measured data are corrected using partial calibration constants for every step of the learning process. As the inversed model the Chebyshew series supplemented by orthogonal correction for small deviations of angles was used:

$$\begin{aligned}
\tilde{x}^k &= F_x T_5 + E_x T_4 + D_x T_3 + C_x{}^k T_2 + B_x T_1 + A_x{}^k T_0 \\
\tilde{y}^k &= F_y T_5 + E_y T_4 + D_y T_3 + C_y{}^k T_2 + B_y T_1 + A_y{}^k T_0 + O_{yx} x^k \\
\tilde{z}^k &= F_z T_5 + E_z T_4 + D_z T_3 + C_z{}^k T_2 + B_z T_1 + A_z{}^k T_0 + O_{zy} y^k + O_{zx} x^k
\end{aligned} \tag{3}$$

Where $T_0 - T_5$ is expansion to Chebyshew series and A, B, C, D, E, F and O are coefficient which the neural network are trying to learn. First six series of Chebyshews polynomials for x – channel:

$$\begin{aligned}
T_5 &= 16\left(x^k\right)^5 - 20\left(x^k\right)^3 + 5\left(x^k\right)^1 \\
T_4 &= 8\left(x^k\right)^4 - 8\left(x^k\right)^2 + 1 \\
T_3 &= 4\left(x^k\right)^3 - 3\left(x^k\right)^1 \\
T_2 &= 2\left(x^k\right)^2 - 1 \\
T_1 &= x^k \\
T_0 &= 1
\end{aligned} \tag{4}$$

The learning process of calibration constants is based on the gradient methodology, thus application of the absolute differential on the error equation (2), resulting into iterative equation, based on which corrected values of the measured orthogonal decomposition of the field vector in the each step are calculated. The same equations for channel y and are defined. We can use expansion to higher series using the recurrence formula:

$$T_{n+1}(x) = 2xT_n(x) - T_{n-1}(x) \tag{5}$$

The learning process of the linearity calibration constants of 5. series *Fx*, *Fy* and *Fz* is based on following equations:

$$\begin{aligned}
F_x{}^{k+1} &= F_x{}^k + 2\tilde{x}^k \alpha \varepsilon^k \left(16\left(x^k\right)^5 - 20\left(x^k\right)^3 + 5\left(x^k\right)\right) \\
F_y{}^{k+1} &= F_y{}^k + 2\tilde{y}^k \alpha \varepsilon^k \left(16\left(y^k\right)^5 - 20\left(y^k\right)^3 + 5\left(y^k\right)\right) \\
F_z{}^{k+1} &= F_z{}^k + 2\tilde{z}^k \alpha \varepsilon^k \left(16\left(z^k\right)^5 - 20\left(z^k\right)^3 + 5\left(z^k\right)\right)
\end{aligned} \tag{6}$$

where α constant influences stability and velocity of the learning process convergence. Similarly for calibration constants of 4. series *Ex*, *Ey* and *Ez*

$$\begin{aligned}
E_x{}^{k+1} &= E_x{}^k + 2\tilde{x}^k \alpha \varepsilon^k \left(8\left(x^k\right)^4 - 8\left(x^k\right)^2 + 1\right) \\
E_y{}^{k+1} &= E_y{}^k + 2\tilde{y}^k \alpha \varepsilon^k \left(8\left(y^k\right)^4 - 8\left(y^k\right)^2 + 1\right) \\
E_z{}^{k+1} &= E_z{}^k + 2\tilde{z}^k \alpha \varepsilon^k \left(8\left(z^k\right)^4 - 8\left(z^k\right)^2 + 1\right)
\end{aligned} \tag{7}$$

For *Dx*, *Dy* and *Dz* calibration constants:

$$
\begin{aligned}
D_x^{k+1} &= D_x^{k} + 2\tilde{x}^k \alpha \varepsilon^k \left(4\left(x^k\right)^3 - 3\left(x^k\right)^1\right)\\
D_y^{k+1} &= D_y^{k} + 2\tilde{y}^k \alpha \varepsilon^k \left(4\left(y^k\right)^3 - 3\left(y^k\right)^1\right)\\
D_z^{k+1} &= D_z^{k} + 2\tilde{z}^k \alpha \varepsilon^k \left(4\left(z^k\right)^3 - 3\left(z^k\right)^1\right)
\end{aligned}
\tag{8}
$$

For *Cx*, *Cy* and *Cz* calibration constants:

$$
\begin{aligned}
C_x^{k+1} &= C_x^{k} + 2\tilde{x}^k \alpha \varepsilon^k \left(2\left(x^k\right)^2 - 1\right)\\
C_y^{k+1} &= C_y^{k} + 2\tilde{y}^k \alpha \varepsilon^k \left(2\left(y^k\right)^2 - 1\right)\\
C_z^{k+1} &= C_z^{k} + 2\tilde{z}^k \alpha \varepsilon^k \left(2\left(z^k\right)^2 - 1\right)
\end{aligned}
\tag{9}
$$

Sensitivity calibration constants marked as $B_x$, $B_y$ and $B_z$ can be calculated using equations:

$$
\begin{aligned}
B_x^{k+1} &= B_x^{k} + 2\tilde{x}^k \alpha \varepsilon^k x^k\\
B_y^{k+1} &= B_y^{k} + 2\tilde{y}^k \alpha \varepsilon^k y^k\\
B_z^{k+1} &= B_z^{k} + 2\tilde{z}^k \alpha \varepsilon^k z^k
\end{aligned}
\tag{10}
$$

For bias calibration constants $A_x$, $A_z$ and $A_z$ we can write equations:

$$
\begin{aligned}
A_x^{k+1} &= A_x^{k} + 2\tilde{x}^k \alpha \varepsilon^k\\
A_y^{k+1} &= A_y^{k} + 2\tilde{y}^k \alpha \varepsilon^k\\
A_z^{k+1} &= A_z^{k} + 2\tilde{z}^k \alpha \varepsilon^k
\end{aligned}
\tag{11}
$$

and orthogonality calibration constants *Ox*, *Oy* and *Oz* can be determined as:

$$
\begin{aligned}
O_{yx}^{k+1} &= O_{yx}^{k} + 2x^k \tilde{y}^k \alpha \varepsilon^k\\
O_{zy}^{k+1} &= O_{zy}^{k} + 2y^k \tilde{z}^k \alpha \varepsilon^k\\
O_{zx}^{k+1} &= O_{zx}^{k} + 2x^k \tilde{z}^k \alpha \varepsilon^k
\end{aligned}
\tag{12}
$$

## 3. MODELING AND SIMULATIONS

For the theoretical principles verification the mathematical model representing random and discrete sensor rotation in the homogeneous field with the defined bias, sensitivity, linearity and orthogonality errors of the simulated measured values was created. The learning process of bias, sensitivity, linearity and orthogonality calibration constants is shown on Fig. 1 – Fig. 7, respectively. The convergence velocity α was set to 0.0003.

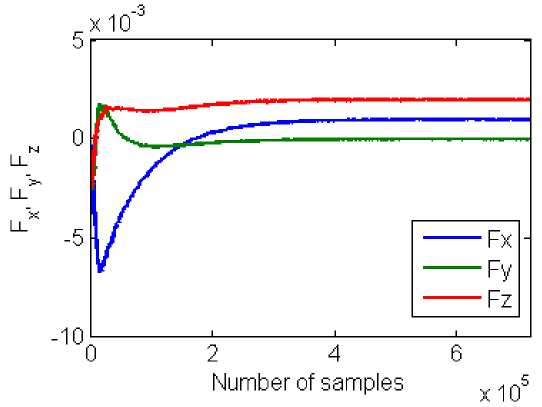


**Figure 1** Learning procces of constant of 5th series

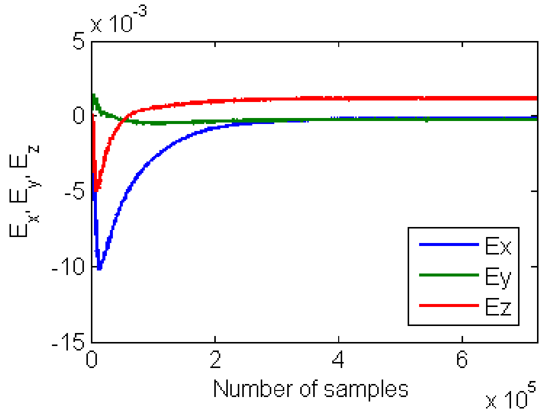


**Figure 2** Learning procces of constant of 4th series

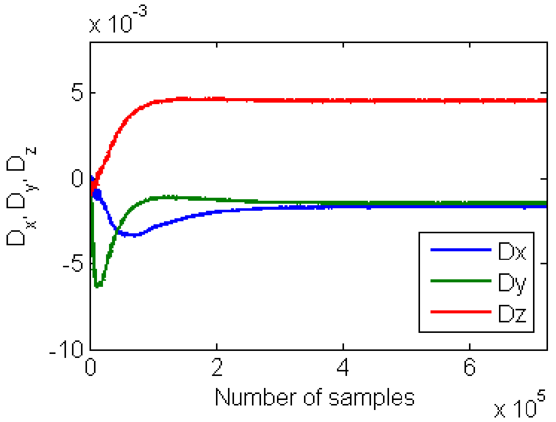


**Figure 3** Learning procces of constant of 3rd series

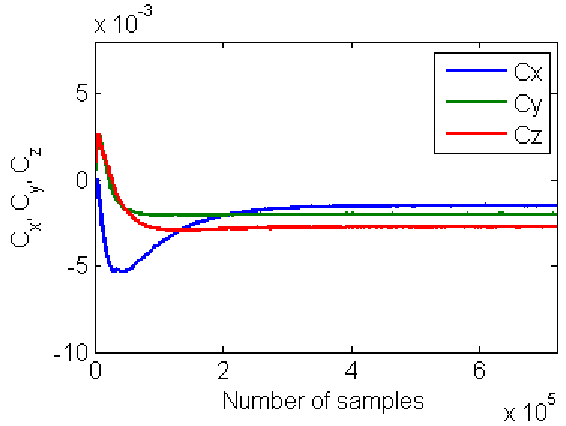


**Figure 4** Learning procces of constant of 2nd series

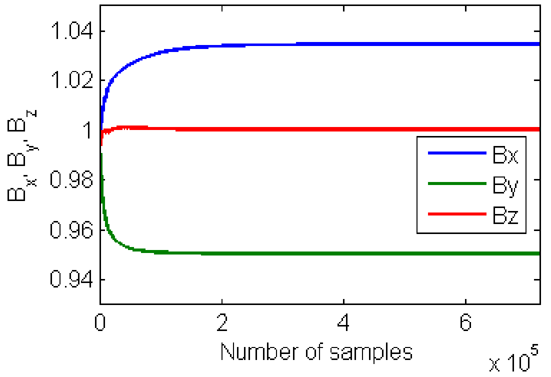


**Figure 5** Learning procces of sensitivity calibration constants

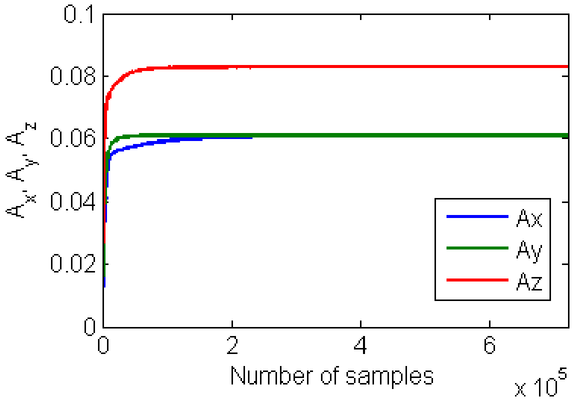


**Figure 6** Learning procces of bias calibration constants

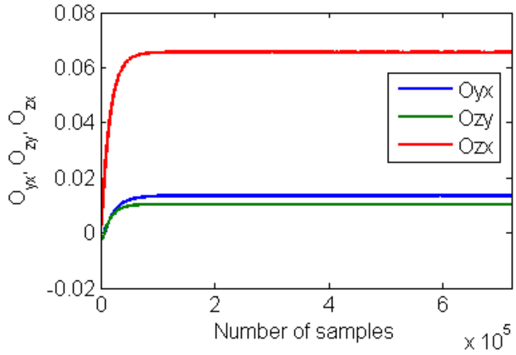


**Figure 7** Learning procces of orthogonality calibration constants

From the illustrated learning processes it is obvious that the most time consuming is the learning process of the calibration constants of the highest order, in our case of the constant of the 2nd, 3rd, 4th and 5th order corresponding to the nonlinearity elimination. The velocity of the sensor calibration is therefore dependent on the velocity of the learning process of this constant. On the other hand the main error sources have an origin in the sensor's bias and sensitivity errors and therefore as can be seen on Fig. 8, which illustrates error calculated from the measured data in comparison with the error calculated after calibration constants application, the error during the learning process achieves the steady state already before the steady state of linearity calibration constants' steady state achievement.

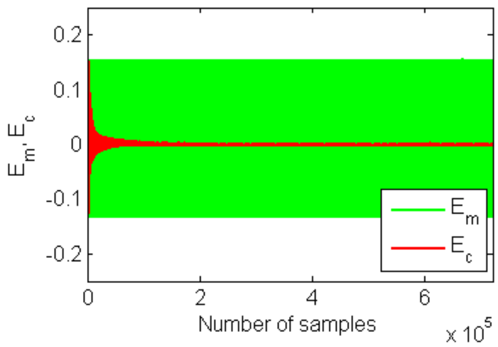


**Figure 8** Comparison of errors calculated from measured data and during the learning process

From the picture we can see that the error calculated from simulated uncalibrated data $\varepsilon_m$ varies from -0.1327 to 0.155 and during the calibration process after stable stated is achieved the error $\varepsilon_c$ is reduced, it varies from -0,0015 to 0.0012, which means a significant improvement of the modeled sensor's characteristics. Moreover the calculated standard deviation of the simulated uncalibrated data with the value of 0.0721 was suppressed during the learning process to the value of 0.00048. In this case, the error was suppresed about 150 times.

## 3. EXPERIMENT

As the simulation results confirmed correctness of this calibration methodology, experimental measurements were performed using the 3-axis simultaneous relax-type fluxgate Vema magnetometer with the resolution of 2 nT [6]. The sampling frequency during the measurements was 1 kHz and each sample was obtained as an average consisting of 20 samples. Measured data were subsequently normalized to 1. Samples was randomized and set of training data was created. The learning process of bias, sensitivity, linearity and orthogonality calibration constants during the measurement is shown on Fig. 9 – Fig. 15, respectively. The convergence velocity $\alpha$ was set to 0.0003.

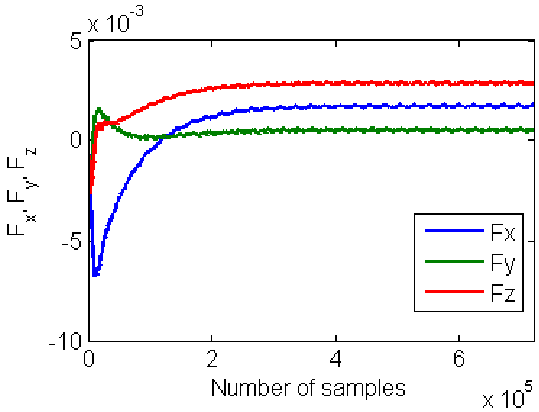


**Figure 9** Learning procces of constant of 5th series

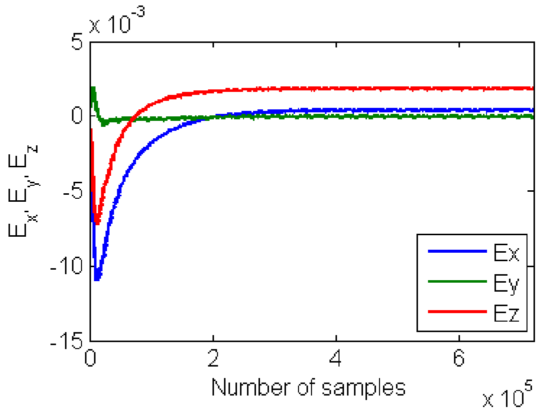


**Figure 10** Learning procces of constant of 4th series

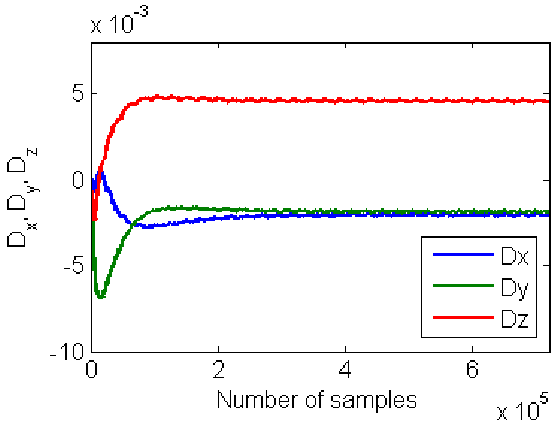


**Figure 11** Learning procces of constant of 3rd series

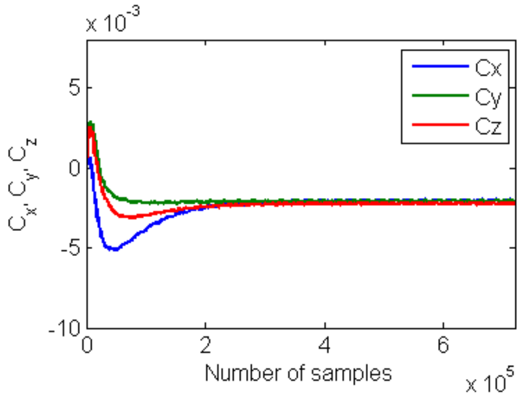


**Figure 12** Learning procces of constant of 2nd series

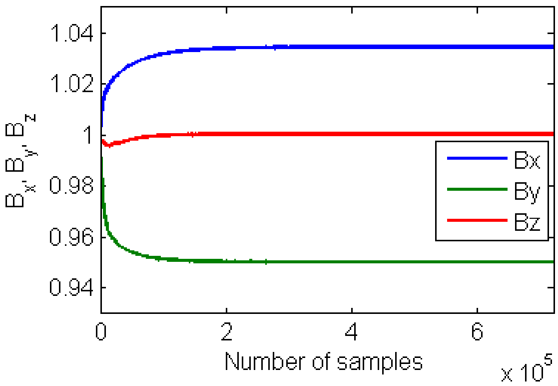


**Figure 13** Learning procces of sensitivity calibration constants

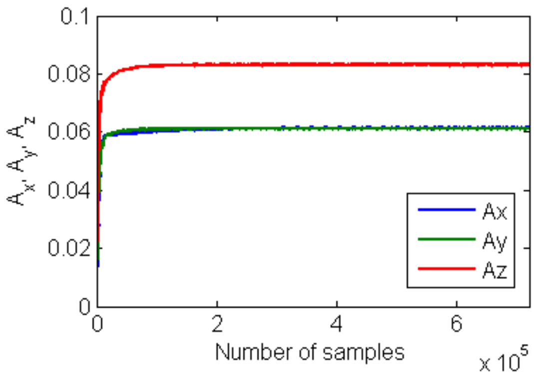


**Figure 14** Learning procces of bias calibration constants

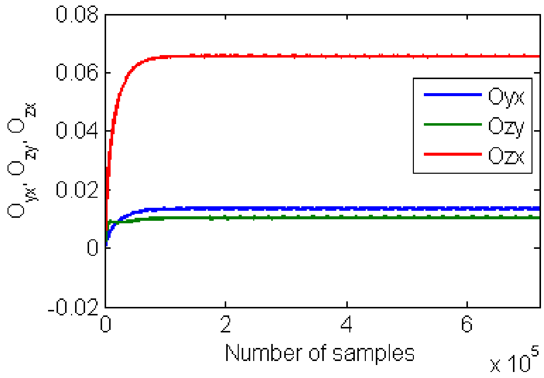


**Figure 15** Learning procces of orthogonality calibration constants

From the illustrated learning processes it is obvious that the most time consuming is the learning process of the calibration constants of the highest order. The overall velocity of the sensor calibration is therefore dependent on the velocity of the learning process of these constants.

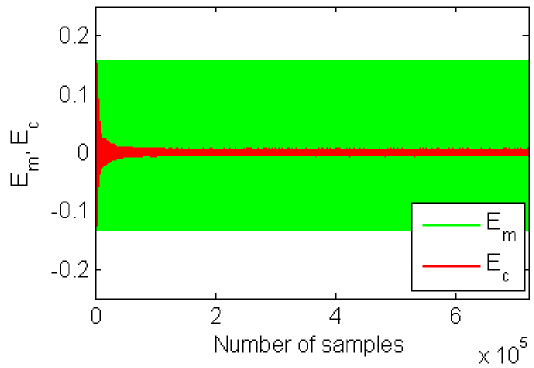


**Figure 16** Comparison of errors calculated from measured data and during the learning process

Fig. 16 illustrates error calculated from the measured data in comparison with the error calculated during the calibration process. Also in this case we can see a significant improvement of the sensor's precision, because the error of the measured data $\varepsilon_m$ changes from -0.133 to 0.158 and after the stable state achievement the error $\varepsilon_c$ changes only from -0.0059 to 0.0053. The standard deviation of the scalar value $T$ was from the value of 3.405 μT eliminated to 0.078 μT. During the experiment, the error was suppresed more than 43 times.

**Table 1** Overview of calibration constants

| Axis | F | E | D | C |
|---|---|---|---|---|
| X | 0.00174 | 0.0004 | -0.00211 | -0.00206 |
| Y | 0.00052 | -0.00005 | -0.00187 | -0.00207 |
| Z | 0.00286 | 0.00182 | 0.00452 | -0.00224 |

**Table 2** Overview of calibration constants

| Axis | B | A | O |
|---|---|---|---|
| X | 0.06137 | 1.03453 | - |
| Y | 0.06114 | 0.95012 | 0.0135 |
| Z | 0.08323 | 1.00036 | 0.0104<br>0.0655 |

Tab. 1 nad 2 summarizes calculated calibration constants of the tested Vema magnetometer. The deviations from the steady state during the calibration process of this relax-type magnetometer were probably caused by the inhomogeneity and non-stationarity of the magnetic field, because measurements were performed in the outdoor conditions without utilization of the magnetic shield chamber. Other measurement errors can have an origin in the axial asymmetry of used ferro probes and in the cross-axis effect.

## 5. CONCLUSION

The theoretical principles of the adaptive attitudeindependent calibration methodology for 3-axis sensors of vector physical fields calibration based on the one-layer feedforward neural network consisting of three adaptive elements was confirmed by the simulation, during which a very good convergence and calibration constants' estimation was achieved. Simulation results were supplemented by the experimental measurements, which also proved the correctness of the proposed calibration algorithm. Finally it can be concluded that the main advantages of the presented calibration methodology lie not only in the simplicity of the calibration algorithm, attitude independency of the sensor during the calibration measurements, no need of non-magnetic calibration platform utilization, but also in the calibration speed, precision and undemandingness leading to the effective magnetometer calibration constants determination and calibration errors reduction.

## 4. LITERATURE LIST

### References

**Journals:**

[1] S.A.H. Tabatabaei, A. Gluhak, R. Tafazolli, "A fast calibration method for triaxial magnetometers," *IEEE Transactions on Instrumentation and Measurement*, Vol. 62, Issue 11, 2013, p. 2929-2937. ISSN 00189456. DOI: 10.1109/TIM.2013.2263913.

[2] R. Alonso, M.D. Shuster, "Complete linear attitude-independent magnetometer calibration," *Journal of the Astronautical Sciences*, Vol. 50, Issue 4, 2003, p. 477-490. ISSN 00219142.

[3] V. Renaudin, M.H. Afzal, G. Lachapelle, "Complete triaxis magnetometer calibration in the magnetic domain," *Journal of Sensors*, Vol. 2010. ISSN 1687-725X. DOI: 10.1155/2010/967245.

[4] H. Pang, D. Chen, M. Pan, S. Luo, Q. Zhang, J. Li, F. Luo, "A new calibration method of three axis magnetometer with nonlinearity suppression," *IEEE Transactions on Magnetics*, Vol. 49, Issue 9, 2013, p. 5011-5015. ISSN 0018-9464. DOI: 10.1109/TMAG.2013.2259842.

[5] H. Pang, J. Li, D. Chen, M. Pan, S. Luo, Q. Zhang, F. Luo, "Calibration of three-axis fluxgate magnetometers with nonlinear least square method," Measurement: *Journal of the International Measurement Confederation*, Vol. 46, Issue 4, 2013, p. 1600-1606. ISSN 0263-2241. DOI: 10.1016/j.measurement.2012.11.001.

[6] J. Blažek, J. Hudák, D. Praslička, „A relax type magnetic fluxgate sensor," *Sensors and actuators A: Physical*, Vol 59, Issue 1-3, 1997, p. 287-291. ISSN 0924-4247.

**Conference Proceedings:**

[7] V. Petrucha, P. Kaspar, "Calibration of a triaxial fluxgate magnetometer and accelerometer with an automated non-magnetic calibration system," *Proceedings of IEEE Sensors*, 2009, p. 1510-1513. ISBN 978-142444548-6. DOI: 10.1109/ICSENS.2009.5398466.